JOURNAL OF CATALYSIS 150, 421–429 (1994)

# Role of Lewis Acidity in the Isomerization of *n*-Pentane and *o*-Xylene on Dealuminated H-Mordenites

Y. Hong, V. Gruver, and J. J. Fripiat[1]

*Department of Chemistry and Laboratory for Surface Studies, P.O. Box 413, University of Wisconsin-Milwaukee, Milwaukee, Wisconsin 53201*

Received May 23, 1994; revised August 19, 1994

*n*-Pentane and *o*-xylene isomerizations have been studied at 285 and 150°C, respectively, on seven dealuminated H-mordenites containing different amounts of framework and nonframework aluminum which were prepared by steaming or calcining $NH_4$-mordenite. The number of Brønsted and Lewis sites were known beforehand from $^{29}Si$ high-resolution magnetic resonance and infrared study of low-temperature CO adsorption. In addition, the availability of the acid sites to the reactants was estimated from the ratios of the liquid monolayer volume of the reactant (*n*-pentane or *o*-xylene) to that of $N_2$, the availability of the active sites to $N_2$ and CO being the same. It was observed that the initial rates of isomerization divided by the number of available Brønsted sites are proportional to the number of available Lewis sites. This observation suggests a synergistic enhancement of the acidity by the interaction between Brønsted and Lewis acid centers. Other aspects related with the products distribution are also discussed.



## INTRODUCTION

The mechanisms of hydrocarbon transformation in zeolites have been reviewed extensively because of the fundamental and economical interest for the petroleum industry (1, 2). While hydrocarbon chemistry in zeolites is widely recognized to be carbocation chemistry, there are questions about how carbenium ions are generated, the nature of their interaction with the zeolite lattice, and their reactivity toward the reactants.

Partially because the nature of Lewis sites in zeolites is not well understood, their role appears not as important, unless their interaction with the Brønsted site is considered. It is well documented that under mild steaming conditions new catalytic sites (enhanced activity sites) are generated in H–ZSM-5 (3–7). The concentration in Brønsted sites is decreased while the number of Lewis acid centers is increased during such a treatment. Lunsford *et al.* (9, 10) observed that a H–Y sample with its full proton loading was relatively inactive in acidity-dependent reactions such as cumene dealkylation and hexane cracking, but when the same material was dehydroxylated at elevated temperature, steamed, treated with $SiCl_4$ (9, 10), or exchanged with $La^{3+}$ (11), considerably more active catalysts were obtained. Using the treatment of ammonium hexafluorosilicate (AHF), and keeping the level of nonframework aluminum relatively low, Beyerlein *et al.* (12) observed that the catalyst exhibited much less carbonium ion activity for isobutane conversion than expected, based on the number of framework aluminum atoms. When the sample was mildly steamed, the activity became considerately greater. Bursian *et al.* (13) found that upon increasing the fluorine content in mordenites, the number of Brønsted sites, determined by the FTIR studies of CO adsorption, decreased while the number of Lewis sites went through a maximum. Meanwhile the catalytic activity for pentane isomerization also went through a maximum. All these observations suggested that Lewis acid sites, eventually related to the nonframework aluminum species, participate in the acidity-dependent reactions on zeolites.

The role of Lewis acid sites in hydrocarbon transformations is not clear. Kazansky *et al.* (3, 4) suggested that Lewis sites would abstract $H_2$ or small alkane molecules (methane, for example) from the alkane and the olefin would thereafter be protonated into a carbenium cation. Beyer (8) considered as a two-center mechanism the reaction whereby the reactant is absorbed on a Lewis site and dehydrogenated at this site, while cracking follows the formation of the carbenium cation resulting from the capture of the proton from a neighboring Brønsted site.

The other possible role of Lewis acid sites stem from their interaction with Brønsted centers. This hypothesis is, however, controversial. Lunsford (11) believed that the isolated nonframework aluminum species generated by steaming or thermal activation, and polyvalent cations formed by ion-exchanging, enhanced the electron withdrawal from the framework hydroxyl groups, making the proton more mobile. Such a push–pull mechanism may be considered as the result of a synergistic interaction.

[1] To whom correspondence should be addressed.



0021-9517/94 $6.00

Hence, the activity for hexane cracking increases with the increasing number of nonframework aluminum. Lago *et al.* (6) and Ashton *et al.* (14) reported similar enhancement of framework Brønsted sites. Beyerlein (12) concluded from the enhancement of isobutane transformation that the enhanced acidity was a result of interaction between the framework Brønsted centers and Lewis centers associated with extraframework aluminum. In 1981, Barthomeuf (15) already suggested this kind of synergism between Lewis and Brønsted sites.

One reason for the uncertainty about the mutual role of both kinds of acid sites may be due to the timing of the events. The adsorption of the reactant must result in a redistribution of charge and energy among the paraffin molecule and the surface site. The enhancement of the proton acidity by the neighboring Lewis site is likely to be modified by the reactant adsorption on the Lewis site or the protonation by the Brønsted site. Then, depending upon the sequence of the events, the role of one site may dominate the role of the other. In the Lewis center–reactant interaction mode the adsorption will lower the energy of proton transfer, or the enhancement of the protonic activity by the neighboring Lewis site is such that the protonation is faster.

Whatever the role of the Lewis acid site is, three issues have to be considered:

(1) The distribution of the framework aluminum causing the enhancement of the strength of the remaining acid sites (this effect is supposed to be only important in the early stage of dealumination of Y zeolite and H-mordenite, or more pronounced in the low Si/Al range) (16).

(2) The overall concentration of Brønsted acid centers.

(3) The amount of nonframework aluminum, which will change the amount of the Lewis acid site concentration and eventually their proximity to the Brønsted sites.

Two reactions were chosen in this work to study the catalytic activity of the dealuminated acid mordenites, namely the isomerization of *o*-xylene and *n*-pentane. The secondary process in the isomerization of xylene is the disproportionation into toluene and trimethylbenzenes. The isomerization of *n*-pentane is always accompanied by cracking and disproportionation.

Thus, the aim of the paper is to clarify as much as possible the respective role of the Brønsted and Lewis site in these reactions. The literature contains scarce quantitative information regarding the number of Lewis acidic centers, and the relationship between the catalytic activity and the surface concentrations of both Brønsted and Lewis acid centers on the zeolite catalyst. This is attributed to the difficulty in estimating the contribution of the Lewis sites and in identifying the nature of these sites. Thus, we will emphasize the different techniques used here to characterize the acidity.

## EXPERIMENTAL

### *Material*

The parent mordenite sample is a commercial product of Union Carbide, Linde Division (LZ-M-5, sodium form). It was exchanged four times with 1M $NH_4NO_3$ at 90°C with solution/solid ratio being 15 ml/g. The sample was then washed with distilled water five times and dried at 120°C for 2 h. The ammonium mordenite was heated up to 250°C at 5°C per minute and kept for 2 h at 250°C in order to remove the adsorbed water. The temperature was increased to 500°C at 5°C per minute and kept at 500°C for 2 h. This sample is the new parent H-mordenite Zeolite, VG2. VG3 is obtained by steaming VG2 at 500°C. $N_2$ with relative humidity 20 Torr $H_2O$/1 atm $N_2$ was passed over the sample for 1 h. Another sample was obtained by steaming VG2 at 600°C. The sample was washed first with 1 *M* HCl at room temperature for 1 h, and then with distilled water and dried. It is labeled VG5. VG400, VG600, VG700, and VG800 were obtained by calcining the dried ammonium mordenite($NH_4M$) for 2 h at 400, 600, 700, and 800°C, respectively.

Thus, we have six samples with the same aluminum content obtained either by calcining $NH_4M$ at 400, 600, 700, and 800°C or by steaming VG2 at 500°C (VG3) and 600°C (VG5). VG5 will have a somewhat lower Al content because of an acid treatment. The reason for the acid treatment was the observation of a huge reduction of the surface area for the sample resulting from steaming at 600°C.

It should be noted that before any catalytic run or acidity measurement, the samples were pretreated for 2 h at 450°C in 760 Torr $O_2$ and degassed for 2 h at the same temperature. In order to avoid further dealumination, VG400 was pretreated at 350°C. Before carrying out the adsorption isotherm measurements, the samples were degassed at 300°C.

### *Catalysts Characterization*

The compositions of the catalysts are shown in Table 1. The ratio Si to framework aluminum ($Si/Al_F^{IV}$) and the ratio Si to total aluminum $(Si/Al)_{CA}$ were obtained from $^{29}Si$ MAS NMR and chemical analyses, respectively. From these ratios and the chemical composition, the absolute numbers of framework aluminum, necessarily in tetrahedral coordination $Al_F^{IV}$, and of the nonframework aluminum, were easily obtained. It was observed that the fraction of noneframework aluminum (NFAl) with respect to the total aluminum was between 4.6% (VG400)

TABLE 1

**Composition of the Dealuminated Mordenites**

| Sample | $Si/Al_{CA}$ | $Si/Al_F^{IV}$ | $Al^t$ ($\times 10^{21}$/g) | $Al_F^{IV}$ ($\times 10^{21}$/g) | $Al_{NF}$ ($\times 10^{21}$/g) | $Al_{NF}/Al_t$ (%) |
|---|---|---|---|---|---|---|
| VG2 | 5.2 | 9.8 | 1.6 | 0.93 | 0.67 | 42.6 |
| VG3 | 5.2 | 11 | 1.6 | 0.84 | 0.76 | 48.3 |
| VG5 | 6.4 | 28 | 1.4 | 0.35 | 1.05 | 74.5 |
| VG400 | 5.2 | 5.5 | 1.6 | 1.54 | 0.07 | 4.6 |
| VG600 | 5.2 | 10 | 1.6 | 0.91 | 0.69 | 43.6 |
| VG700 | 5.2 | 15 | 1.6 | 0.63 | 0.99 | 61.3 |
| VG800 | 5.2 | 111[a] | 1.6 | 0.09 | 1.5 | 94.5 |

*Note.* $Si/Al_{CA}$ and $Si/Al_F^{IV}$ are the ratios obtained from chemical analysis and $^{29}Si$ MAS NMR, respectively. $Al^t$, $Al_F^{IV}$ are the absolute Al total contents and framework Al contents per gram of dehydrated zeolites samples (300°C), respectively. $Al_{NF}/Al_t$ is the fraction of Al in nonframework position.

[a] $Si/Al_F^{IV}$ ratios larger than 50 are very uncertain. It would correspond to a 4Q (Si–1–Al) contribution smaller than 3% of the total integrated intensity of the $^{29}Si$ signal.

and 75% (VG5). VG800 was higher but as indicated in Table 1 the ($Si/Al_F^{IV}$) result for this sample was uncertain.

The measurement of the unit cell parameters and crystallinity was performed using a Scintag diffractometer, $CuK_\alpha$ radiation. The lengths of the *a*, *b*, *c* parameters are shown in Table 2 as well as the volume = *a*b*c* of the unit cell, in agreement with references (18, 19). The sum of the intensities of the 111, 130, 241, 002, 511, and 530 diffractions was used to calculate the degree of crystallinity of the samples with respect to the ammonium exchanged mordenite (18), taken as reference (100%). It was observed that despite deep lattice dealumination in VG5 and VG800, more than 80% of the starting crystallinity were retained.

*Adsorption Studies*

Three adsorbates were chosen to study the adsorption properties of the samples: $N_2$, pentane and benzene. $N_2$ is the classical probe for surface area and pore size distribution measurements, and, what is more important, $N_2$ has the same molecular size as CO, which implies that all the acid centers measured by CO adsorption FTIR are also accessible to $N_2$. Because of its very low vapor pressure, the adsorption isotherms of *o*-xylene cannot be measured easily at room temperature; benzene was used instead to mimic the behavior of *o*-xylene.

$N_2$ adsorption–desorption isotherms were measured with an Omnisorp 100 in the static mode at liquid nitrogen temperature. All isotherms leveled out from P/Po = ~0.01 up to P/Po = ~0.8, that is up to the onset of the capillary condensation on external surfaces. The specific surface areas shown in Table 3 are the Langmuir surface areas. They seem independent of the dealumination of the mordenite. The *n*-pentane and benzene adsorption isotherms were measured at room temperature with the same automated instrument; they looked like Brunauer

TABLE 2

**Unit Cell Parameters *a*, *b*, *c***

| Sample | *a* (Å) | *b* (Å) | *c* (Å) | Volume (Å$^3$) | Crystallinity (%) | $Al_F^{IV}$/UC | $Al_{NF}$/UC |
|---|---|---|---|---|---|---|---|
| VG2 | 18.06 ± 0.01 | 20.42 ± 0.02 | 7.49 ± 0.01 | 2764.27 | 91 | 4.44 | 3.20 |
| VG3 | 18.12 ± 0.04 | 20.41 ± 0.07 | 7.47 ± 0.02 | 2761.95 | 90 | 4.00 | 3.63 |
| VG5 | 18.11 ± 0.04 | 20.27 ± 0.07 | 7.43 ± 0.02 | 2727.02 | 81 | 1.67 | 5.02 |
| VG600 | 18.05 ± 0.04 | 20.30 ± 0.07 | 7.44 ± 0.02 | 2725.46 | 86 | 4.36 | 3.30 |
| VG700 | 18.04 ± 0.03 | 20.27 ± 0.05 | 7.43 ± 0.01 | 2717.90 | 82 | 3.00 | 4.74 |
| VG800 | 17.94 ± 0.03 | 20.18 ± 0.04 | 7.41 ± 0.01 | 2682.06 | 82 | 0.43 | 7.18 |

*Note.* The crystallinity was obtained from the sum of the intensities of the 111, 130, 241, 002, 511, and 530 diffraction lines. The original $NH_4$ mordenite is taken as reference at 100% crystallinity. Volume is the unit cell volume a*b*c. $Al_F^{IV}$/UC and $Al_{NF}$/UC are the numbers of framework and nonframework Al per unit cell, respectively.

TABLE 3

S. A. is the Langmuir Surface Area Measured by $N_2$ Adsorption at Liquid Nitrogen Temperature

| Sample | S.A. ($m^2/g$) | S.A. (m + M) ($M^2/g$) | S.A. (m + M)/S.A. (%) | $V_m$ (ml/g) | $V_{m\text{-}C5}/V_m$ (%) | $V_{m\text{-}benz}/V_m$ (%) |
|---|---|---|---|---|---|---|
| VG2 | 463.6 | 28.0 | 6.03 | 0.1654 | 13.05 | 11.13 |
| VG3 | 500.3 | 37.8 | 7.56 | 0.1776 | 18.23 | 13.51 |
| VG5 | 451.8 | 50.7 | 11.2 | 0.1618 | 12.71 | 10.31 |
| VG400 | 488.0 | 28.7 | 5.88 | 0.1731 | 29.70 | 23.01 |
| VG600 | 470.5 | 34.9 | 7.42 | 0.1702 | 28.09 | 22.56 |
| VG700 | 470.0 | 38.7 | 8.23 | 0.1691 | 17.33 | 17.21 |
| VG800 | 438.5 | 39.4 | 8.99 | 0.1555 | 16.20 | 10.29 |

*Note.* S.A. (m + M) is the surface area in the mesopores (2–30 nm in diameter) and macropore (>30 nm in diameter) and S.A. (m + M)/S.A. is the fraction with respect to the total surface area. $V_m$ is the monolayer volume of liquid nitrogen. $V_{m\text{-}C5}/V_m$ and $V_{m\text{-}benz}/V_m$ are the ratios of either the monolayer volume of liquid pentane or of liquid benzene to the monolayer volume of liquid nitrogen.

Type II isotherms. Pentane and benzene adsorption isotherms are shown in Figs. 1 and 2.

For comparing the adsorption of very different gases on a microporous solid, the best was to compare the filling of the porosity at a relative pressure when the capillary condensation on outside surfaces could still be neglected. According to the Gurvitch rule (20), the volumes of condensed liquids should be the same, as observed, for instance, for the NBS alumina standard (with a BET $N_2$ surface area equal to 158 $m^2/g$). At P/Po = 0.92, the volume of liquid pentane (0.385 ml/g) represented 94% of the volume filled by liquid nitrogen (0.411 ml/g), see Fig. 3a.

However, in the dealuminated mordenites about 42 to 54% of the volume filled by $N_2$ was filled by pentane at P/Po = 0.9, while the ratios of the volumes at the completion of the monolayer were between 10 and 30% of the corresponding $N_2$ volumes, see Fig. 3b. The possible explanations for the apparent failure of the Gurvitch rule are: (i) the nonaccessibility of a fraction of the pores created by a partial blockage by the nonframework alumina debris, (ii) the difference in the kinetic diameters of $N_2$ (~3.5 Å), *n*-pentane (~4.5 Å), and benzene (5.5 ~ 6 Å) (1) and the inaccessibility of the 8-member-ring channels for *n*-pentane and benzene (CO and $N_2$ were accessible to these channels).

The reduction in the molecular traffic as well as the decrease in the availability of the active sites were kept in mind in the interpretation of the catalytic activity results. It should be pointed out, as shown elsewhere (21), that the reductions of the adsorption capacity for *n*-pentane or benzene compared to $N_2$ are particular to dealuminated mordenite. We did not observe it to such an extent in acid Y zeolites or ZSM-5 (around 20% drop in availability (21) for both Y zeolites and ZSM-5).

### *Surface Acidity*

As explained in detail elsewhere (17), semiquantitative measurements of the concentrations of Brønsted and Lewis sites were carried out using FTIR spectroscopy of CO chemisorbed at low temperature. As abundantly doc-

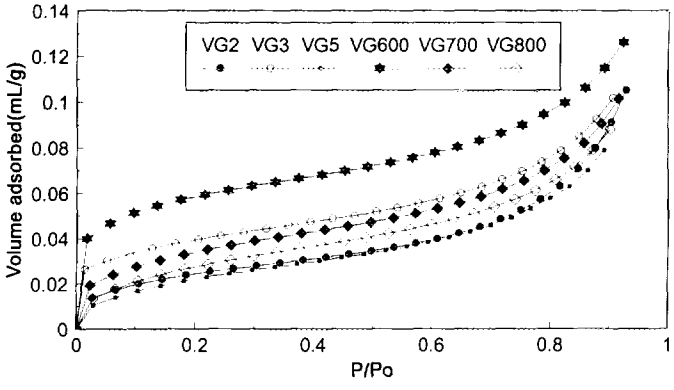


FIG. 1. Pentane adsorption isotherms on dealuminated H-mordenites (295 K). Volume adsorbed is converted to volume of liquid pentane.

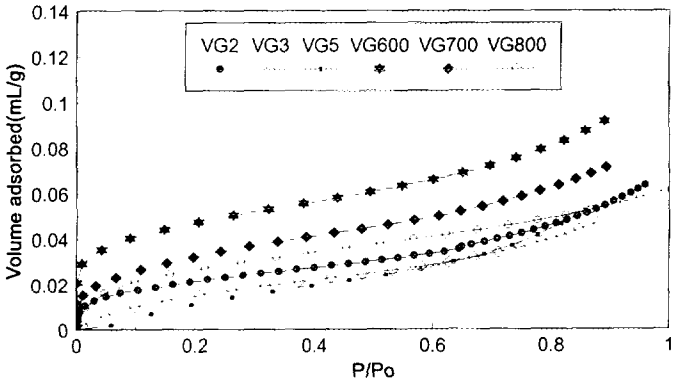


FIG. 2. Benzene adsorption isotherms on the same mordenites (295 K). Volume adsorbed is converted to the volume of liquid benzene.

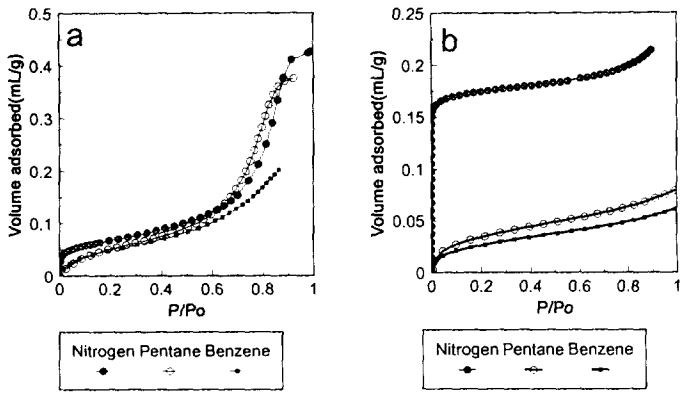


FIG. 3. Comparison of the adsorption isotherms of $N_2$, pentane, and benzene on NBS alumina (158 $m^2/g$) (a) and VG3 (b). Volume adsorbed expressed as the volume of the condensed liquid.

umented and reviewed briefly in Ref. (17), three kinds of acid sites were detectable in this way. The Brønsted sites corresponding to the lattice Si–OH–Al bridging OH showed up as a CO vibration at 2170 $cm^{-1}$. The two strong Lewis sites were identified by CO vibrations at 2218 ± 2 $cm^{-1}$ (L2) and 2193 ± 3 $cm^{-1}$ (L1), respectively. A chemisorption energy of 40.8 kJ/mol was associated to the former while it was 27.1 kJ/mol for the latter, which indicated that there was stronger interaction between the Lewis acid center and CO than that between Brønsted center and CO molecule. The physical adsorption energy which was in the order of 9 kJ/mol was not included in these values. Unfortunately, the adsorption of CO did not provide direct information on the acid strength of the Brønsted sites. The semiquantitative contents in Brønsted and Lewis acid sites are shown in Table 4.

*Catalytic Activity Procedure*

The isomerization of *o*-xylene was carried out in a recirculation system with a total volume of 1.35 l. *o*-Xylene (3 Torr) in the system were mixed with helium so that the total pressure was 1 atm. *o*-Xylene (95% + purity, Eastman Kodak) was dried on activated 4A zeolite and further purified by several freezing–thawing cycles. No significant amount of impurities was observed by gas chromatography. The reactions were performed at 150°C and the composition was analyzed *in situ* by gas chromatography (Perkin-Elmer 8500 with the Alltech column 8453PC 812091L 2077A 6 ft × 1/6 in. × .085 in. s.s. p/w).

The isomerization of pentane was also carried out in the same recirculation system. Pentane (50 Torr) (EM Science, 98%+) in the whole system was mixed with $H_2$ to bring the total pressure to 1 atm. Pentane was dried on activated 4A zeolite and further purified by several freezing–thawing cycles. The main impurity was about 0.5% isopentane. A column from Alltech Co. (C-5000 986714L SN#9308A 20 ft × 1/8 in. × 0.085 in. s.s. p/w V-7 60/80 mesh) was used to identify the reaction products.

TABLE 4

**Number of Brønsted Sites (B), Lewis Acid Sites $L_1$ and $L_2$**

| Sample | VG2 | VG3 | VG5 | VG400 | VG600 | VG700 | VG800 |
|---|---|---|---|---|---|---|---|
| B | 11.0 | 7.4 | 3.2 | 13.0 | 8.7 | 6.8 | 0.9 |
| $L_1$ | 0.92 | 1.2 | 0.40 | — | 1.1 | 0.92 | 0.88 |
| $L_2$ | 0.43 | 0.53 | 0.26 | — | 0.48 | 0.57 | 0.54 |
| $L_1 + L_2$ | 1.4 | 1.7 | 0.66 | 0.6 | 1.6 | 1.5 | 1.4 |
| Dispersion (%) | 20.9 | 22.3 | 6.3 | 86 | 23.2 | 15.1 | 9.3 |

*Note.* Unit $10^{20}$ sites per gram of dehydrated material. Margin of relative uncertainty: ~10%. Dispersion (%) is the percent ratio (L1 + L2)/NFAl, from Table 1.

## RESULTS AND DISCUSSION

It is believed that the nonframework aluminum moieties in zeolites are the source of Lewis acidity which is supported by our results (17, 25). The number of Lewis acid centers did not depend only on the absolute number of nonframework aluminum atoms, but also on the dispersion of the nonframework alumina species and on the aluminum coordination. From our FTIR studies (17), the number of Lewis acid centers could be up to about one order of magnitude less than the number of nonframework aluminum atoms. Specifically, what Table 4 told us was that the ratio L1/L2 did not vary much. A particular interesting point appeared also by comparing (L1 + L2) in Table 3 with NFAL in Table 1. Between 5 to 85% of the NFAl were Lewis sites, and since only a fraction of the subsurface Al atoms were L1 or L2 sites, the NFAl debris must be highly dispersed. A high degree of dispersion should favor the interaction between Lewis and Brønsted sites by decreasing the average distance between them.

The number of framework aluminum atoms per unit cell decreased with the severity of the dealumination obtained either by steaming or by calcination, while the unit cell volume decreased, as shown in Table 2. Since mordenite is orthorhombic (19), the parameters *a*, *b*, *c*, corresponding to the dimension of three lattice axes, may change differently. Guisnet *et al.* (22) observed heterogeneous changes in offretite, another orthorhombic zeolite. From VG2 to VG800, parameter a changed by approximately 0.6% among the samples, while parameter *b* and *c* changed by ~1.2 and 1.1%, respectively.

As reported in the literature, dealumination of zeolites through hydrothermal (steaming) treatment promotes the formation of a mesoporous structure (23, 24). According to Table 3, the $N_2$ surface areas did not change appreciably, but the fraction of surface area in mesopores and

macropores, obtained from *t*-plots, increased slightly with the number of NFAl. All this structural and textural information was condensed in Figs. 4a and 4b.

In Fig. 4a, the decrease of the unit cell volume with the decrease in the number of $Al_F^{IV}$ per unit cell seemed to be linear. This approximation was better for the thermally treated samples, VG600, VG700, and VG800 than for the steamed samples VG2, VG3, and VG5. The two kinds of treatments have obviously different effects on the unit cell volume. The physical reason for the difference between these treatments was unknown but it also affected the increase in the fraction of the surface area in the meso- + macropores (m + M) as shown in Fig. 4b. While steaming has a weaker effect on the dimensions of the lattice parameters than the thermal treatment, it increased more rapidly the nonmicroporous volume contribution.

However, whatever the nature of the treatment, more than 88% of the pore volume measured by $N_2$ are still in the micropore range, in agreement with the high residual crystallinity. There observations cannot be reconciled easily with the poor availability to *n*-pentane and benzene. This difficulty was specially high for VG400. The amount of nonframework aluminum in VG400 was much less than in VG600, but the sites' availability, either Vm–C5/Vm or Vm–ben/Vm, were the same, namely 30 and 23%, respectively. Thus, the blockage of the pores by alumina debris was hardly the major factor restricting the availability of the active sites. The possibilities that remain are: (i) that the kinetic diameter was a main factor, and (ii) that lattice dislocations affected the pore connectivity. Indeed, the nature of the treatment played a role, since steaming (VG2, VG3, VG5) restricted the availability more than the thermal treatment (VG400, VG600, VG700, VG800). This observation corroborated what is shown in Fig. 4b, namely that the thermal treatment did not change the meso- and macroporosity. As shown in Table 4, the dispersion of the alumina debris also depended on the nature of the treatment. Therefore, besides physical restriction due to the lack of availability of a fraction of the porous structure and of the catalytic sites, the degree of dispersion of the NFAl should play a role if the Lewis sites were implied in the reactions studied here.

TABLE 5

**Rate-Iso. and Rate-crack. Are the Initial Rates for Isomerization and Cracking of Pentane, Rate-Iso. and Rate-disp. Are the Initial Rate of Isomerization and Disproportionation of *o*-Xylene. Units: Molecule Transformed per Minute on 1 Gram of Catalyst**

| | *o*-Xylene, 150°C | | Pentane, 285°C | |
|---|---|---|---|---|
| Sample | Rate-Iso. ($\times 10^{16}$) | Rate-Disp. ($\times 10^{16}$) | Rate-Iso. ($\times 10^{14}$) | Rate-crack. ($\times 10^{14}$) |
| VG2 | 6.5 | 3.0 | 2.7 | 1.4 |
| VG3 | 8.0 | 2.8 | 3.9 | 2.3 |
| VG5 | 0.088 | 0.088 | 0.36 | 0.050 |
| VG400 | — | — | 5.2 | 3.3 |
| VG600 | 4.7 | 1.5 | 1.3 | 8.2 |
| VG2700 | 0.99 | 0.47 | 3.5 | 1.2 |
| VG2800 | 0.040 | 0.066 | 0.64 | 0.65 |

In discussing the mutual role of the Brønsted and Lewis centers, the isomerization of pentane will be considered first, Table 5. We chose to ignore the Lewis sites and to represent (Fig. 5) the variation of the initial rate divided by the number of available Brønsted sites toward the number of framework aluminum atoms per unit cell. Thus, we represented the turnover number (TON) vs the extent of dealumination. This function passed through a maximum. Two cases could be anticipated: either the TON was constant, which meant that the Brønsted sites

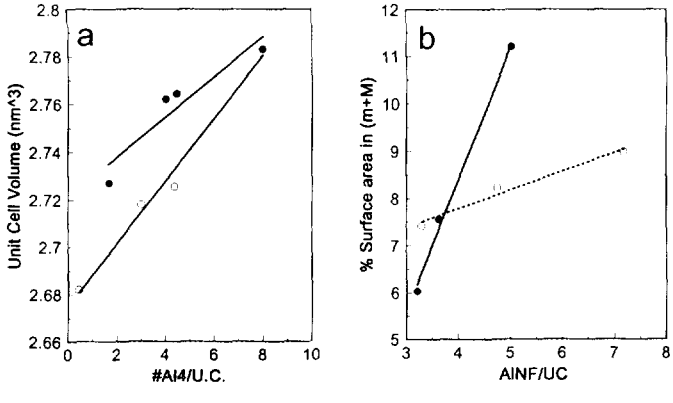


FIG. 4. (a) Relationship between the unit cell volume of mordenite samples and the number of tetrahedral aluminum atoms per unit cell; (b) relationship between the fraction of nonframework alumina and the fraction of the surface area in the mesopore and macropore range ($N_2$ adsorption). Open marker, thermal; filled marker, steaming treatment.

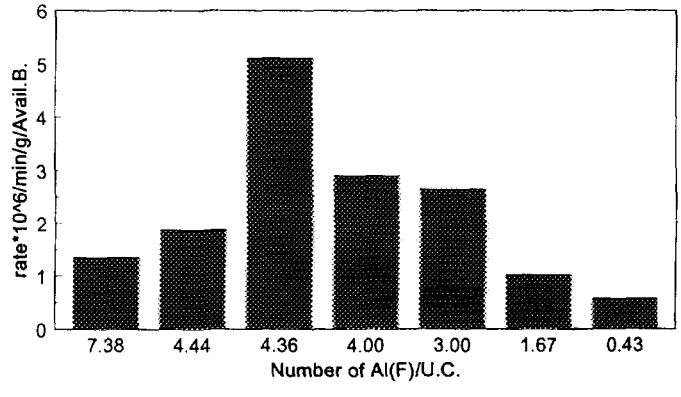


FIG. 5. Relationship between the initial rate of pentane isomerization divided by the number of available Brønsted sites vs the number of framework aluminum atoms per unit cell.

have the same strength, or the strength would increase slightly as a fraction of the framework aluminum was removed (16, 17), then the TON should increase until a plateau is reached. The only explanation for a maximum would be that the strength passed through a maximum as the mordenites were dealuminated. As far as we are aware such maximum has never been documented, so there must be factors other than Brønsted acidity involved in the overall activity.

Note the importance of the sites' availability when comparing the catalytic activity to the acidity. For instance, the ratio $V_{m\text{-}C5}/V_m$ (Table 3) is 13% for VG2 while it is 28% for VG600 in spite of the similar contents in $Al_{NF}$.

Now let us consider Fig. 6 in which the TON is plotted vs the number of available Lewis sites. Six out of seven data points are on a straight line passing near the origin. The lacking data point is that obtained from VG800 in which, as outlined in Table 1, the $Al_F^{IV}$ content can be wrong by a factor of 2. (If it was the case, the data point would not be far from the linear regression!)

Thus, the initial rate of *n*-pentane isomerization appears as the product of the probability that an available Brønsted site is in interaction with the reagent by the probability that this Brønsted site interacts with a Lewis site. The converse is equally probable. This explanation would also support the hypothesis of mutual enhancement of the strength of the Brønsted or of the Lewis acid sites, respectively, by the Lewis or Brønsted site neighbor. What comes first is open to debate. If the Russian school is followed, the Lewis site would be the adsorption site by which the molecule to be transformed is transiting. However, it is not because the heat of chemisorption of CO or of $NH_3$ is higher on a Lewis site than on a Brønsted that the same is true for an alkane. This point will not be discussed further because, so far, there is no valid argument available to reference.

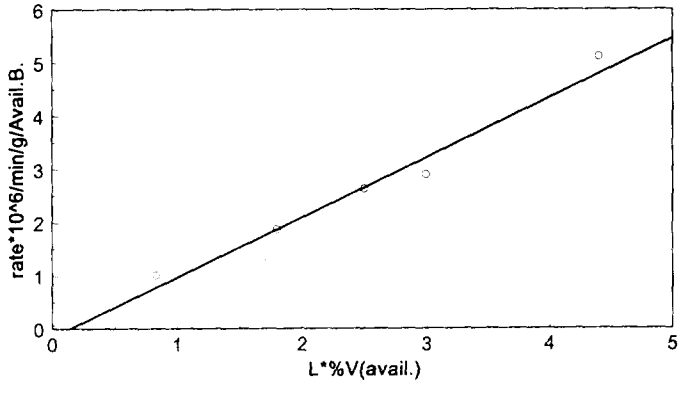


FIG. 6. The linear relationship between the initial rate of pentane isomerization at 285°C per available Brønsted site vs the number of available Lewis site $\times 10^{-19}$.

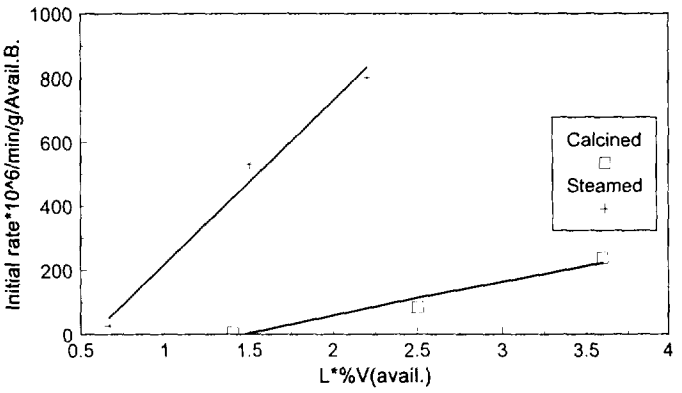


FIG. 7. Same relationship as in Fig. 6 for *o*-xylene isomerization at 150°C. (+) for steamed samples and (□) for calcined samples.

In Fig. 7, we show that the TON for the *o*-xylene isomerization follows a similar trend as that in Fig. 6. In the case of *n*-pentane isomerization, it does not appear that the nature of the treatment, thermal of steaming, matters and the intercept of the linear regression (Fig. 6) is zero. In the case of *o*-xylene isomerization, even though the TON increased with the number of available Lewis centers, different trends were observed for catalysts prepared differently.

The initial rate of isomerization of *n*-pentane was approximately 1.6 times that of cracking, irrespective of the catalyst, while the initial rate of isomerization of *o*-xylene is about 2.7 times that of disproportionation. Because these ratios were almost constant, the nature of the catalytic sites for cracking or disproportionation should be the same as for isomerization. The rate-limiting step should be the same which, in turn, suggests a similar intermediate.

The hydrogen transfer from olefin in the cracking of *n*-pentane seemed to be quite efficient on all our catalysts, since no olefin had been found. The reasons for this observation might be: (i) the relatively low temperature favored the hydrogen transfer, and (ii) olefin was more easily protonated by Brønsted centers than paraffins.

The product distributions after 5% conversion of pentane are shown in Fig. 8 as a function of the nature of the catalysts. The catalysts are ranked according to the number of Brønsted sites and of the preparation procedure: thermal on the left or steaming on the right. Although the differences were weak, it seemed that (i) the relative proportion of *i*-pentane and of C6 increase as the Brønsted acidity decreased and (ii) on the opposite, the relative proportion of (C1 + C2) decreased as the number of Brønsted sites decreased. In Fig. 7, the distribution on VG600 had not been represented, because the first data point corresponded to a higher degree of conversion.

As far as the *o*-xylene transformation was concerned, the selectivity of three concurrent reactions was shown

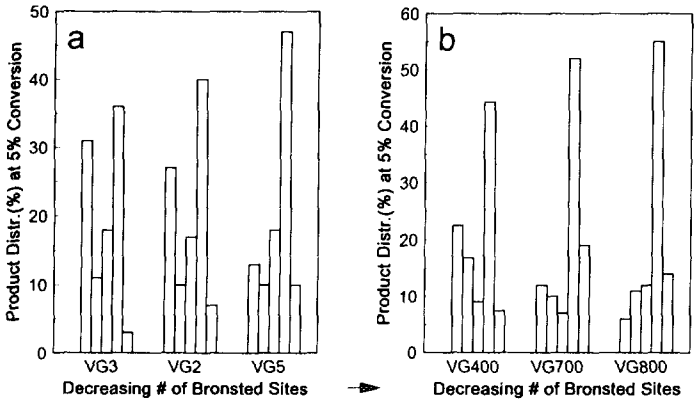


FIG. 8. Products' distribution (%) at 5% conversion of pentane (285°C). From left to right: % ($C_1$+$C_2$); % $C_3$; % $C_4$; % i-$C_5$; % $C_6$. The catalysts are ranked in the order of decreasing contents in Brønsted sites.

in Fig. 9, with respect to the nature of the catalyst treatment. The condensation corresponded to the formation of a colored, probably polyaromatic, residue resulting from the condensation of trimethylbenzene. Here two trends were observable. The selectivity toward isomerization decreased with the decreasing number of Brønsted sites while, accordingly, the selectivity toward condensation increased at the expense of the disproportionation selectivity. Thus, the trends observed for *o*-xylene were opposite to those reported for pentane.

The ratio meta/para xylene at 10% conversion was about 10 for the most active catalysts and larger than 20 on VG5 and VG800.

## CONCLUSIONS

This work illustrates the difficulty of linking the nature of an acid catalyst to its performance in two isomerization reactions, namely, the isomerization of *n*-pentane and that of *o*-xylene. Here the catalysts were H-mordenites either steamed or thermally dehydroxylated. In a separate work, the amount of Brønsted sites (per g of dried catalyst) was obtained from $^{29}$Si MAS NMR while the concentrations in Lewis sites were calculated from the intensity of the two characteristic CO vibrations at ~2190 and 2220 $cm^{-1}$. We showed here that these characterizations must be completed by a correction factor which measured the availability of the Brønsted or Lewis sites to the reactants, *n*-pentane and *o*-xylene. In addition, the nature of the treatment (steaming or thermal activation) had its own importance.

From the relationships between the turnover number per available Brønsted site and the available Lewis centers, a synergistic mechanism apparently existed in both isomerizations of pentane and *o*-xylene.

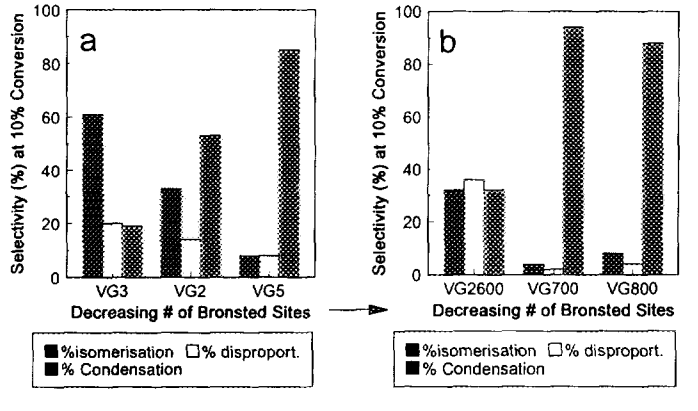


FIG. 9. Selectivity of isomerization, disproportionation, and condensation reactions at 10% conversion of *o*-xylene at 150°C.

## ACKNOWLEDGMENTS

The financial support of DOE Grant DT-FG02-90 ER1430 is gratefully acknowledged. We also thank Dr. A. Blumenfeld and D. Coster for the NMR data.

## REFERENCES

1. Jacobs, P. A., and Martens, J. A., *in* "Introduction to Zeolite Science and Practice" (H. Van Bekkum, E. M. Flanigan, and J. C. Jansen, Eds.), *Stud. Surf. Sci. Catal.*, Vol. 58. Elsevier, Amsterdam, 1991.
2. Poutsma, M. L., *in* "Zeolite Chemistry and Catalysis" (J. A. Rabo, Ed.), Vol. 171, p. 437. ACS Monograph, Washington, D. C., 1976.
3. Zholobenko, V. L., Kustov, L. M., Borovkov, V, Yu., Kazansky, B. V., *Kinet. Katal.* **128,** 965 (1987).
4. Zholobenko, V. L., Kustov, L. M., Kazansky, B. V., Loeffler, E., Lohse, U., and Oehman, G., *Zeolites* **11,** 132 (1991).
5. Topsoe, N.-Y., Joensen, F., and Derouane, E., *J. Catal.* **110,** 404 (1988).
6. Lago, R. M., Haag, W. O., Mikovsky, R. J., Olson, D. H., Hellring, S. D., Schmitt, K. D., and Kerr, G. D. *in* "Proceedings of the 7th International Zeolite Conference" (Y. Murakami *et al.*, Eds.), p. 677. Kodansha, Tokyo, 1986.
7. Luk'yanov, D. B., *Zeolites* **14,** 233 (1994).
8. Beyer, H., *Acta Chim. Acad. Sci. Hung.* **84,** 25 (1975).
9. DeCanio, S. J., Sohn, J. R., Fritz, P. O., and Lunsford, J. H., *J. Catal.* **101,** 132 (1986).
10. Sohn, J. R., DeCanio, S. J., Fritz, P. O., and Lunsford, J. H., *J. Phys. Chem.* **90,** 4847 (1986); *J. Catal.* **125,** 123 (1990).
11. Carvajal, R., Chu, Po-Jen, and Lunsford, J. H., *J. Catal.* **125,** 123 (1990).
12. Beyerlein, R. A., McVicker, G. B., Yacullo, L. N., and Ziemiak, J. J., *J. Phys. Chem.* **92,** 1967 (1988).
13. Bursian, N. R., Botutsky, P. N., Georgiesky, V. Yu, Gruver, V. Sh, Krasii, B. V., Lastovkin, G. A., Martynova, G. B., Orlov, D. S., and Brovko, V. N., *Prepr. Am. Chem. Soc. Div. Pet. Chem.* **36(4),** 893 (1991).
14. Ashton, A. G., Batmanian, S., Clark, D. M., Dwyer, J., Fitch, F. R., Hinchdtle, A., and Mochado, F. J., *in* "Catalysis by Acid and Bases" (B. Imelik *et al.*, Eds.), p. 101. Elsevier, Amsterdam, 1985.

15. Mirodatos, C., and Barthomeuf, D., *J. C. S. Chem. Commun.* 39 (1981).
16. Anderson, M. W., and Klinoski, J., *Zeolites* **6,** 455 (1986).
17. Gruver, V., and Fripiat, J. J., *J. Phys. Chem.* **98,** 8549 (1994).
18. Chumbhale, V. R., Chandwadkar, A. J., and Rao, B. S., *Zeolites* **12,** 63 (1992).
19. Meier, W. M., and Olson, D. H., "Atlas of Zeolite Structure Types" 3rd ed. Butterworth-Heinemam, 1992.
20. Gregg, S. J., and Sing, K. S., "Adsorption, Surface Area and Porosity." Academic Press, New York, 1982.
21. Hong, Y., Gruver, V., and Fripiat, J. J., in preparation.
22. Brotas de Carvalho, M., Carvalho, A. P., Ramoa Ribeiro, F., Florentino, A., Gnep, N. S., and Guisnet, M., *Zeolites* **14,** 217 (1994).
23. Fernandez, C., Vedrine, J. C., Grosmangin, J., and Szabo, G., *Zeolites* **6,** 484 (1986).
24. Zukal, A., Patzelova, V., and Lohse, U., *Zeolites* **6,** 133 (1986).
25. Coster, D., Blumenfeld, A., and Fripiat, J. J., *J. Phys. Chem.* **98,** 6201 (1994).
26. Macedo, A., Auroux, A., Raatz, F., Jacquinot, E., Boulet, R., "Perspectives in Molecular Sieve Science" (W. H. Flank and T. W. Whyte, Jr., Eds.), Vol. 116, p. 98. JACS Symposium Series 368, American Chemical Society, Washington, D. C., 1988.
27. Thomas, C. L., "Catalysis Processes and Proven Catalysts." Academic Press, New York, 1970.
28. Ruthven, D. M., "Principles of Adsorption and Adsorption Process." Wiley, New York, 1984.
29. Beschmann, K., and Rickert, L., *J. Catal.* **141,** 548 (1993).
30. Corma, A., Faraldos, M., and Mifsud, A., *Appl. Catal.* **47,** 125 (1989).
31. Hruzik, D., Krupcik, J., and Leclercq, P. A., *Zeolites* **10,** 213 (1990).
32. Haag, W. O., and Dessau, R. M., "Proceedings, 8th International Congress on Catalysis, Berlin, 1984." Dechema, Frankfurt-am-Main, 1984.